Planar anchoring and surface melting in the smectic-*A* phase

Emmanuelle Lacaze,[1,*] Jean-Philippe Michel,[2] Michel Alba,[3] and Michel Goldmann[1]
[1]*INSP, CNRS UMR-7588, Universités Pierre et Marie Curie-Paris 6, 140 Rue de Lourmel, F-75015 Paris, France*
[2]*CRPP, CNRS UPR-8641, avenue Paul Schweitzer, F-33600 Pessac, France*
[3]*LLB, UMR12 CEA-CNRS, CEA-Saclay, F-91191 Gif-sur-Yvette Cedex, France*
(Received 15 November 2006; published 5 October 2007)

We study ultrathin films of 8CB in planar anchoring on a MoS_2 inorganic substrate. We evidence an anchoring breakage for 60-nm-thick films, in favor of the homeotropic anchoring at the air interface. This allows one to determine the 8CB-MoS_2 smectic anchoring energy. We then demonstrate for films thinner than 60 nm that, under the homeotropic bulk, an intermediate film remains in planar anchoring, associated with a melting of the smectic layers close to the substrate. Such a melting could be general for planar or tilted anchorings and we show that, for strong anchorings, the anchoring energy can be driven by the deformations of this intermediate nematic film.

DOI: 10.1103/PhysRevE.76.041702 PACS number(s): 61.30.Hn, 61.10.−i, 68.35.Bs, 68.35.Md

I. INTRODUCTION

The phenomenon of liquid crystal (LC) anchoring is not fully understood, despite years of studies conducted by many groups all over the world. In the nematic phase the major influence of the interface roughness [1] and/or of the LC molecules physisorbed at the interface [2,3] is now established. However, the nature of the intermediate film which connects the interface to the nematic bulk remains mainly unknown. This film, hidden by the LC bulk and by the substrate, is extremely difficult to observe. No prediction about the anchoring energy can then be obtained on a given system, even if the anchoring directions and their connection with the interface nature are determined, since the anchoring energy value is directly connected to the intermediate film structure.

In the smectic phase, the nature of the intermediate film is also unknown. However, even the issue of the specificity of the smectic anchoring with respect to the nematic one remains regularly addressed. Some observations suggest intrinsic differences between both anchorings: in the homeotropic geometry, wetting phenomena of the smectic phase within the nematic one are observed for flat interfaces [4]. A particular high value of the anchoring energy has been measured [5]. On the contrary, the anchorings of nematic and smectic phases appear similar in the planar anchoring geometry, at least associated with similar orientations of the director with respect to the interface [3,6,7]. This could finally suggest a specificity of the smectic anchoring for appropriate geometries only.

In this context, we focused on planar smectic anchoring and induced an anchoring breakage in ultrathin films. This allowed one to reveal the nature of the intermediate film closed to the substrate, in connection with the value of the anchoring energy. Our results highlight a way for LC systems in the smectic phase to deal with planar anchorings: the melting of the smectic layers at the interface. Our results also show that, in case of strong anchoring, the smectic anchoring energy can be driven by the deformations of the nematic film, close to the LC-substrate interface.

II. EXPERIMENT

The system is a smectic 8CB film, spin-coated on a MoS_2 substrate whose preparation has been previously described [3,8]. A strong multistable planar anchoring is imposed to the nematic and smectic-*A* 8CB phases on MoS_2, due to the presence of the ordered interface on the substrate. This anchoring leads to the presence of large domains in the 8CB film due to six possible planar orientations of the director, each domain being unidirectionally anchored on the 8CB-substrate interface [3].

In films thinner than 350 nm, because the 8CB-air interface imposes a homeotropic anchoring, antagonistic to the planar one, each domain relaxes in well-ordered oily streaks. These oily streaks are flattened hemicylinders (quarters of cylinders joined by parallel layers flat on the substrate) [Fig. 1(a)]. They are associated with two kinds of defects, walls between two quarters of cylinders [arrows W in Fig. 1(a)], characterized by the top angle θ, and disclinations at the curvature centers of the quarters of cylinders [arrows RGB in Fig. 1(a)] [8,9]. Optical microscopy (OM) performed under crossed polarizers reveals the presence of the ribbons of flat layers joining the quarters of cylinders [Fig. 1(b)]. Atomic force microscopy (AFM) reveals the undulations of the upper 8CB-air interface [Fig. 2(a)]. X-ray diffraction reveals continuous rotation of the smectic layers if one aligns the scattering plane parallel to the hemicylinders axis. This corresponds to a domain specific diffraction of the smectic layers. After geometrical corrections (the background is subtracted, the evolution of the beam footprint and of the penetration depth leading to a transmission factor step are taken into account [8]), the Bragg intensity becomes proportional to the number of smectic layers oriented with the director parallel to the wave vector. The wave-vector orientation and such the measured director orientation with respect to the substrate is defined by α [Fig. 1(a)]. The layers rotate in quarters of cylinders, from a perpendicular orientation on the substrate ($\alpha=0°$) to a parallel one ($\alpha=90°$), leading to a

*emmanuelle.lacaze@insp.jussieu.fr

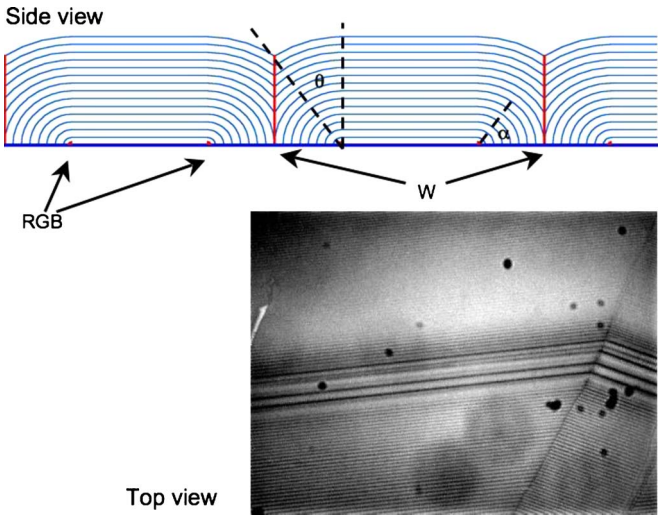

FIG. 1. (Color online) Side view (in the plane perpendicular to the hemicylinders axis): oily streaks in flattened hemicylinders, associated with disclinations [lines at the curvature centers of the quarters of cylinders (RGB arrow)], conjugated with walls [between two quarters of cylinders (W arrow)]. α is the angle between the smectic layers director and the substrate surface, varying between 0° and 90°, θ is the wall top angle. Top view: optical microscopy image (160×120 μm^2) between crossed polarizers (polarizer orientation horizontal) of a 200-nm-thick 8CB film on MoS_2 with two domains of different planar unidirectional anchorings. The largest domain is divided in two homogeneous parts of thickness 200 nm (at the top of the image and at the bottom) with quasiperiodic black ribbons of period of the order of 1.4 μm, associated with the flat layers joining the quarters of cylinders. In the middle, a thicker area displays larger hemicylinders.

constant intensity between $\alpha=0°$ and 80°, as shown in Fig. 3 for a 450–nm-thick film (around $\alpha=90°$ the diffraction of flat layers is measured) [8,10]. Although the disclinations appear in thick films as straight lines lying flat on the substrate, they possess a three-dimensional structure [10]. They are half tube-shaped rotating grain boundaries (RGB) of spatial extension about 110×140 nm^2, partitioning the parallel smectic layers from the rotating ones [Fig. 4(a)]. Due to the presence of the disclinations, when the thickness becomes smaller than 140 nm, the film turns into an extremely constrained structure. The RGBs geometry suggests indeed that the film structure is described by quasiperpendicular layers separated from parallel ones by the remaining portion of RGB [Fig. 4(b)]. This is demonstrated by x-ray results for $e=70$ nm (Fig. 3), leading to a Bragg intensity, only associated with layers rotating between $\alpha=0°$ and 25° and with flat layers ($\alpha=90°$).

III. RESULTS: ANCHORING BREAKAGE

For ultrathin films of thickness, e, smaller than a critical value, $e_c\approx60$ nm, the experimental data are dramatically modified: the ribbons in OM images disappear and the images become perfectly homogeneous. The 8CB-air surface undulations observed by AFM also disappear. At 85 nm they are only partly detected [Fig. 2(b)] and no longer at 60 nm. On a sample of thickness $e=50$ nm, at room temperature ($T=23$ °C), no rotation of the smectic layers is observed by x-ray diffraction, contrary to higher thicknesses. The signal from flat layers (rising at $\alpha=90°$) is still observed in this sample (Fig. 3), which indicates that parallel smectic layers are preserved in ultrathin films. However, this signal could also be associated with the presence of flattened hemicylinders oriented along one of the five other possible orientations on the substrate, as the peak rising at $\alpha=90°$ integrates the signal of the flat layers belonging to all the domains of the liquid crystal film illuminated by the x-ray beam, whatever their orientation with respect to the x-ray beam. It is then interesting to follow the evolution with temperature of a very thin film, far from the smectic-nematic transition (33.5°). Figure 5 presents such an x-ray evolution for a 70-nm-thick film. Rotating smectic layers are still detected at small α, for $T=23$ °C, but are no longer detected for $T=27$ °C (between $\alpha=0°$ and 30°), whereas the signal coming from the flat layers (at $\alpha=90°$) has proportionally diminished but is still clearly detected. This result cannot be interpreted as a change of orientation of the hemicylinders: No signal is measured at ±5° if the sample is azimuthally tilted. Moreover, the OM measurements do not show any disorientation with the temperature between the different possible planar anchoring orientations on the substrate, in agreement with the observed stability up to 120 °C of the underlying 8CB-substrate interface [11] and in agreement with the observation of strictly equivalent planar anchorings in the smectic and nematic phases [3]. However, OM data evidence, for $T=27$ °C, a disappearance of the ribbons already for a thickness of $e_c\approx80$ nm. These results demonstrate finally the disappearance of the oily streaks and the transformation of the smectic film into a homogeneous homeotropic one, for $e_c\approx80$ nm at $T=27$ °C. The similarity of the film's structure for $e\approx60$ nm at $T=23$ °C strongly suggests that the same homogeneous homeotropic film is formed for $e\approx60$ nm at $T=23$ °C and therefore that an anchoring breakage occurs at critical thicknesses varying with temperature.

IV. EVALUATION OF THE SMECTIC ANCHORING ENERGY

This anchoring breakage corresponds to the transformation of a deformed smectic film into an undeformed one with an *a priori* disadvantageous homeotropic anchoring on the substrate. It is characterized by the transformation of the quarters of cylinders into flat layers parallel to the substrate. We can then restrain on a given quarter of cylinder of height e and lateral extension L (Fig. 4) to describe the anchoring breakage from an energetic point of view.

The energy of a quarter of cylinder per unit of length is

$$E_Q = E_{S1} + E_{el} + E_{S2} + E_{RGB} + 1/2E_W. \quad (1)$$

E_{S1} stands for the quarter of cylinder surface energy per unit of length at air, it is proportional to γ_{air}, the surface tension of 8CB at air. E_{el} stands for the rotating layers elastic energy. $E_{S2}=\gamma_{SP}L$ stands for the surface energy per unit of length on MoS_2 with γ_{SP} the surface tension of 8CB in planar anchor-

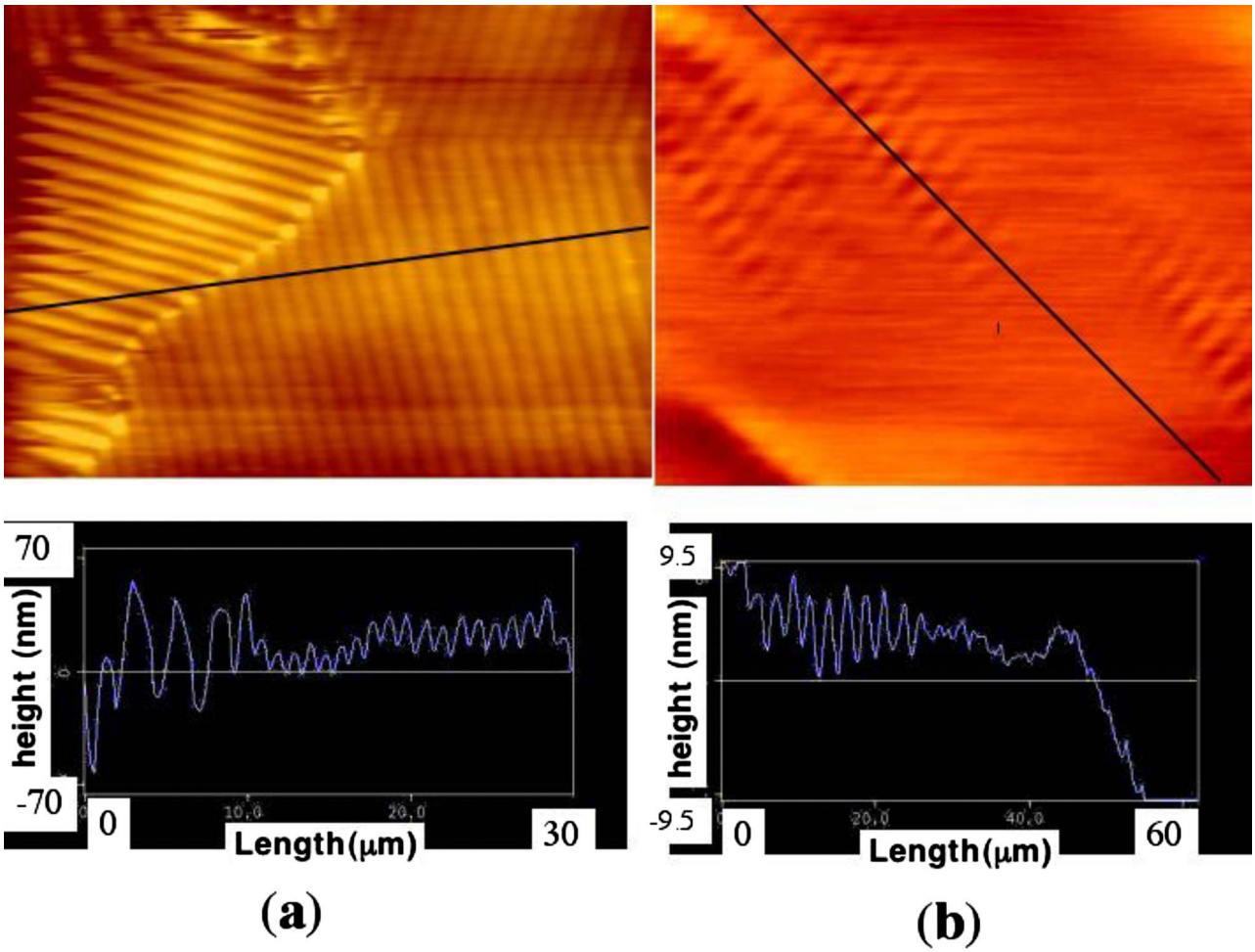

FIG. 2. (Color online) (a) AFM image performed in noncontact mode (30×25 μm^2, height scale 140 nm) of a 160-nm-thick 8CB film on MoS_2 with three domains of different planar unidirectional anchorings. The oily streaks lead to quasiperiodic undulations of the surface. The corresponding height profile is indicated below. (b) AFM image (50×40 μm^2, height scale 19 nm) of a 85-nm-thick 8CB film on MoS_2. Undulations have disappeared in the thinner parts of the surface. The corresponding height profile is indicated below.

ing on MoS_2. E_{RGB} is the RGB energy per unit of length and has been estimated as 4.6×10^{-10} J m$^{-1}\leqslant E_{RGB}\leqslant 1.2\times10^{-9}$ J m^{-1} [10]. E_W is the wall energy per unit of length (shared by two consecutive quarters of cylinders).

We can define the energy per unit of length of flat layers as $E_F=E'_{S1}+E'_{S2}$, with $E'_{S1}=\gamma_{air}L$ and $E'_{S2}=\gamma_{SH}L$, γ_{SH} standing for the surface tension of 8CB in homeotropic anchoring on MoS_2, connected to the smectic anchoring energy, $\Delta\gamma_S$, on MoS_2, as $\Delta\gamma_S=\gamma_{SH}-\gamma_{SP}$.

When the thickness becomes smaller than 140 nm, the energy per unit of length of the RGB becomes dependent on the thickness in a nonlinear way, the energy per unit of surface of the RGB increasing from the top [T in Fig. 4(a)] to the bottom [B in Fig. 4(a)]. Indeed disorientation between the layers separated by the RGB increases from 0° at the top towards 90° at the bottom, close to the 8CB-substrate interface. This finally leads for $T=23°$ C to an anchoring breakage occurring for $e_c\approx60$ nm. 60 nm being 40% of 140 nm, roughly 40% of the RGB perimeter should remain in a 60 nm smectic film [Fig. 4(b)].

The presence of an anchoring breakage shows that $E_Q\leqslant E_F$ for $e\geqslant140$ nm and $E_Q\geqslant E_F$ for $e\leqslant e_c$, so $E_{RGB}+E(e)\leqslant\Delta\gamma_S L$ for $e\geqslant140$ nm and $\beta E_{RGB}+E(e)\geqslant\Delta\gamma_S L$ for $e\leqslant e_c$, with β the ratio between the RGB energy per unit of length at $e=e_c$ and the one at $e=140$ nm, $0.4\leqslant\beta\leqslant1$. $E(e)=E_{el}+1/2E_W+E_{S1}-\gamma_{air}L$. $E(e)=E_{el}+1/2E_W+\gamma_{air}e(\theta-\sin\theta)$ for $e\geqslant140$ nm. $E(e)=E_{el}+1/2E_W+\gamma_{air}(e/\cos\phi)[\theta-2\cos(\phi+\theta/2)\sin(\theta/2)]$ for $e\leqslant e_c$, with ϕ depending on e and being defined by the RGBs geometry, $0\leqslant\phi\leqslant83°$ [Fig. 4(b)].

The knowledge of the RGBs geometry allows us to determine extreme L values, the exact L value depending on the θ value, for a given thickness: For $e=140$ nm, $L\leqslant L_t=140$ nm and for $e=e_c$, $L\geqslant L_c=100$ nm (Fig. 4). We can estimate that $E(e)\approx2\times E(e_c)$ for $e=140$ nm. This leads to

$$\frac{E_{RGB}+2\times E(e_c)}{L_t}\leqslant\Delta\gamma_S\leqslant\frac{\beta E_{RGB}+E(e_c)}{L_c}. \qquad (2)$$

We finally obtain $\beta\geqslant0.7$, in agreement with an RGB energy per unit of length depending on the thickness in a nonlinear way, $0\leqslant E(e_c)\leqslant2/3E_{RGB}$, and

$$3.2\times10^{-3}\text{ J m}^{-2}\leqslant\Delta\gamma_S\leqslant2\times10^{-2}\text{ J m}^{-2}. \qquad (3)$$

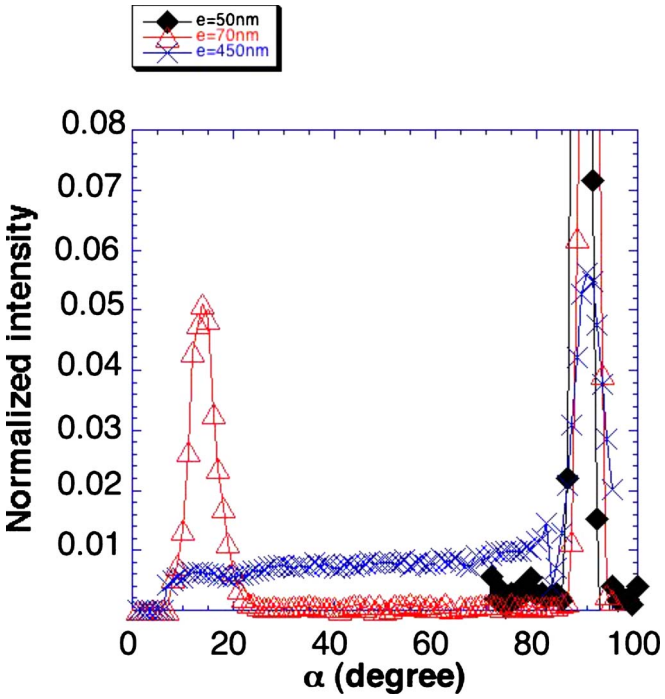

FIG. 3. (Color online) Bragg intensity, proportional to the distribution of smectic layers, versus the orientation of the director with respect to the substrate surface. The intensity is normalized between $\alpha=0°$ and 100°. $e=450$ nm (blue crosses); $e=70$ nm (red open triangles); and $e=50$ nm (black closed squares): no signal is detected between $\alpha=0°$ and 80°, only the signal between $\alpha=70°$ and 100° is consequently presented.

Not only $\Delta\gamma_{MoS_2}$ is higher than 3.2×10^{-3} J m^{-2} but also $\Delta\gamma_{air}$, as the homeotropic anchoring is favored with respect to the planar one. $\Delta\gamma_{air}$ is then higher than $\Delta\gamma_{MoS_2}$. 3.2×10^{-3} J m^{-2} is an extremely high value compared to most anchoring energies of nematic and smectic phases, between 10^{-7} and 10^{-4} J m^{-2} [6,12–15]. For example, $\Delta\gamma_{air}$ of 8CB in the smectic phase appears higher than two orders of magnitude with respect to $\Delta\gamma_{air}$ of 5CB in the nematic phase [12]. This difference should be correlated to the well-known smectic wetting at the homeotropic 8CB-air interface [4]. The value 3.2×10^{-3} J m^{-2} is indeed of the same order of magnitude as a smectic anchoring energy on a lecithin covered ITO substrate, also associated with homeotropic anchoring [5]. The fact that $\Delta\gamma_{air}$ is higher than $\Delta\gamma_{MoS_2}$ can be attributed to the presence of a smectic wetting at air which does not exist on the substrate. However, the fact that both smectic anchoring energies are high addresses the issue of the specificity of the smectic anchoring. The smectic anchoring could indeed lead to particularly high anchoring energies in the case of appropriate geometries, that is homeotropic or planar unidirectional ones.

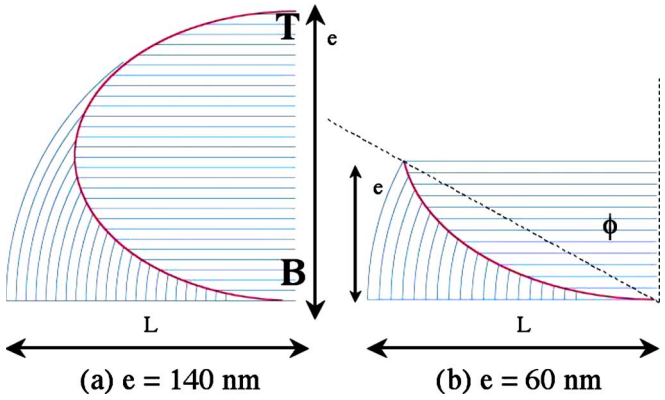

FIG. 4. (Color online) Quarters of cylinders of very thin films. The smectic layers are schematized and the RGB is highlighted with $\phi(e)$, the angle defined by the RGBs profile and depending on e; the wall between the quarters of cylinders is not drawn for the sake of clarity. (a) $e=140$ nm: $\phi=0°$ and (b) $e=60$ nm: $\phi=59°$.

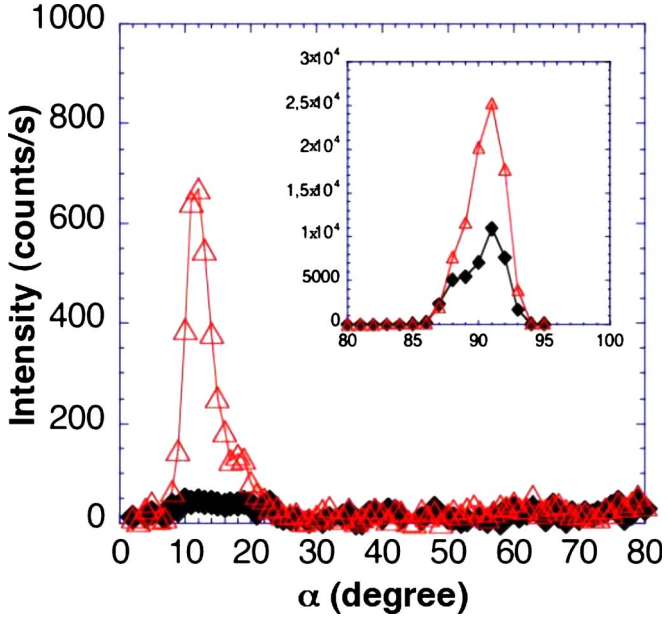

FIG. 5. (Color online) Bragg intensity profile versus α for a 70-nm-thick film for two different temperatures, 23 °C (red open triangles) and 27 °C (black closed squares).

V. MELTING CLOSE TO THE SUBSTRATE

In order to test this specificity, the study of homogeneous ultrathin films in a planar unidirectional geometry is useful: The intermediate film close to the substrate is no more negligible with respect to the bulk and can be revealed through OM studies. In the case of 8CB ultrathin films on MoS_2 (of thickness smaller than 60 nm), OM images are essentially dark between crossed polarizers, as expected for homeotropic films. However, some domains of the LC films appear slightly colored for given orientations of the sample with respect to the analyzers. Although these domains are still visible under exactly crossed polarizers, they can be more clearly observed when the polarizers are slightly uncrossed (Fig. 6). As the entire ultrathin LC films can be similarly lighted by rotating the sample with respect to the polarizers orientation, a nonzero planar projection of the LC director must exist at the 8CB-substrate interface, associated with domains (Fig. 6).

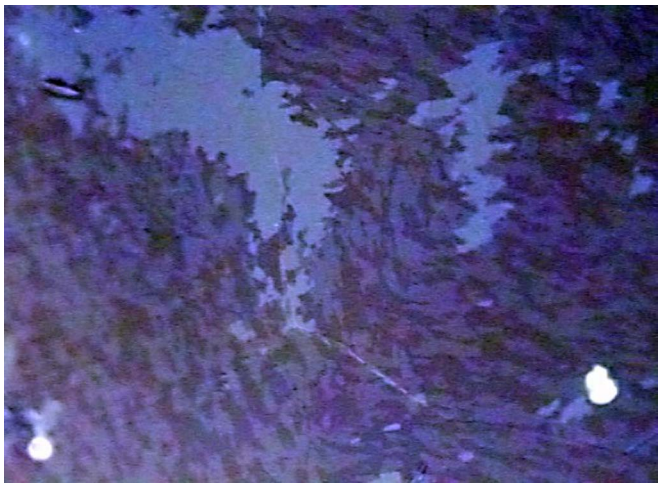

FIG. 6. (Color online) OM image ($400\times300\ \mu m^2$) of a 30-nm-thick 8CB film on MoS_2. Two large domains appear quasi-white under slightly uncrossed polarizers, associated with unidirectional planar anchoring, close to the substrate, at 45° from the polarizers orientations. The domains of different colors correspond to planar anchoring with different orientations (close to parallel to the polarizers for black domains).

On the other hand, whatever the LC film thickness, the planar ordered 8CB-MoS_2 interface is preserved everywhere on the substrate, as observed through STM measurements. Domains in ultrathin LC films are consequently associated with domains of the underlying LC-substrate interface, as it is in thick nematic and smectic films [3]. However, the 8CB-substrate interface is an interfacial 2 to 3 Å thick monolayer [16], too thin to be observed by optical microscopy. This is confirmed by the fact that in LC films, thinner than 20 nm, the presence of the planar domains cannot be revealed despite the presence of the underlying 8CB-MoS_2 interface. Domains in ultrathin LC films are then thicker than the planar 8CB-substrate interfacial monolayer. A prewetting of a three layer 8CB film occurs on silicon substrates, as evidenced by ellipsometry measurements associated with x-ray reflectivity ones [17]. However, such a film cannot account for the optical microscopy observations, since only the first layer in this three layer film possesses a nonzero molecular projection on the substrate. Our domains should therefore correspond to a LC film confined between the ordered planar 8CB-substrate interface and the homeotropic smectic bulk. It has to be distorted to accommodate the planar anchoring on the 8CB-substrate interface and the homeotropic structure of the smectic bulk. It can correspond to smectic-*A* layers strictly perpendicular to the ordered interface, which cannot be detected by x-ray diffraction due to the absence of beam output under the 8CB critical angle. However, a grain boundary, partitioning the perpendicular smectic layers from the parallel ones of the homeotropic bulk, would be of higher energetic cost than disclinations, which have already disappeared in ultrathin films. It can also correspond to a smectic-*C* film of which the period of the layers is different from the smectic-*A* ones and would therefore not be detected by x-ray diffraction. However, similarly to the hypothesis of planar smectic-*A* layers, the connection with the homeotropic smectic-*A* film would not be obvious, since it should again impose the presence of large grain boundaries of high energetic cost. On the contrary, a nematic wetting film under the homeotropic bulk would induce the energetic cost of the melting of smectic layers but its deformations could be of lower energetic cost. Due to the small thickness of the film, the deformations should induce the presence of localized defects [18]. A rough estimation of the associated energy can be obtained using the elastic energy of a deformed nematic film between planar and homeotropic anchoring [19]. It is of the order of $(\pi^2/4)K/d$ with d the nematic thickness. For $d=10$ nm, we obtain an energy of 3×10^{-3} J m^{-2}, the same order of magnitude of the 8CB smectic anchoring energy on MoS_2. This indicates that the value of the smectic anchoring energy can indeed be monitored by the deformations of a nematic film, wetting the 8CB-substrate interface. The smectic anchoring energy corresponds to the deformation of the nematic film but not to its creation: the nematic film can be partially ordered but a rough estimation of the energetic cost of its creation is obtained using a Landau-de Gennes free energy and leads to a value of the order of 3.5×10^{-2} J m^{-2} for a nematic film, 10 nm thick [20], significantly larger than the formerly obtained 8CB-MoS_2 smectic energy. Consequently the nematic wetting should also exist under the smectic layers in planar anchoring and therefore under the thick 8CB films on MoS_2. This means that a melting should occur at the bottom of the oily streaks of Fig. 1 and also at the bottom of the RGB (Fig. 4). The hypothesis of a nematic envelope for the RGB, from the bottom to the top [10], becomes now particularly attractive. Moreover, the anchoring breakage occurring at 60 nm should correspond not only to a transformation of the quarters of cylinders into flat layers but also to a transformation of the nematic film below, from homogeneous planar to hybrid. This coincidence is consistent with the similarity of the values of the estimated smectic anchoring energy and the estimated nematic deformation energy (in ultrathin film). It is interesting to notice that, in the oily streaks, the nematic film at the interface has to be already hybrid below the flat smectic layers joining the quarters of cylinders (Fig. 1).

Such a phenomenon of surface melting is opposite to the well-known smectic wetting in the homeotropic geometry [4] and invalidates the hypothesis of specific smectic anchoring with respect to the nematic one in planar geometry. However, it appears consistent with the general observation of similar smectic and nematic planar anchorings. Surface melting is a well-known phenomenon in solid systems, as in ice systems, for example [21]. It could occur frequently in smectic systems for planar, or tilted anchorings, according to the nontrivial accommodation of the smectic layers with respect to the interface in these geometries. For example, the 8CB-MoS_2 interface is a two-dimensional crystal, in which 8CB molecules are organized in lamellae of period 25 Å, necessitating one dislocation over six smectic layers to accommodate the smectic period 31.6 Å [3]. A nematic film between the smectic layers and the organized interface can then be of lower energetic cost than a direct accommodation of the smectic layers on top of the organized interface. One can also expect such a melting for rough interfaces. This could explain the recent observations of disorder in smectic

films, taking place close to grated glass surfaces [22]. This could also explain the particularly low positional anchoring energy, of the order of 10^{-8} J m^{-2}, associated with a low surface smectic order parameter value, of the order of 10^{-5}, for the system butiloxy-benzylideneoctylaniline (4O.8) on silicon oxide (SiO) substrate, rough because it is evaporated in grazing incidence [23].

Our results also demonstrate that, for strong planar anchorings, the smectic anchoring energy can be driven by the deformations of the nematic film close to the interface. This suggests an evolution of the smectic anchoring energy with the temperature which explains the observation of an anchoring breakage which occurs at critical thicknesses varying with temperature. Such an evolution of the smectic anchoring energy with temperature could constitute an important parameter for the interpretation of smectic-nematic phase transitions in confined systems. Our results finally demonstrate a particularly large nematic anchoring energy of 8CB on MoS_2 which must be larger than 3.2×10^{-3} J m^{-2}. This last result should be related to an also extremely high anchoring energy of 5CB in planar unidirectional anchoring on another crystalline substrate, mica, which displays no anchoring breakage for confinement values as small as 20 nm [24]. This suggests a strong influence of the order of the underlying interface on the values of nematic planar anchoring energies.

[1] D. Berreman, Phys. Rev. Lett. **28**, 1683 (1972).
[2] X. Zhuang, L. Marrucci, and Y. R. Shen, Phys. Rev. Lett. **73**, 1513 (1994).
[3] E. Lacaze, J. P. Michel, M. Goldmann, M. Gailhanou, M. de Boissieu, and M. Alba, Phys. Rev. E **69**, 041705 (2004).
[4] B. M. Ocko, X. Z. Wu, E. B. Sirota, S. K. Sinha, O. Gang, and M. Deutsch, Phys. Rev. E **55**, 3164 (1997).
[5] Z. Li and O. D. Lavrentovich, Phys. Rev. Lett. **73**, 280 (1994).
[6] B. Jérôme, Rep. Prog. Phys. **54**, 91 (1991).
[7] P. Hubert, H. Dreyfus, D. Guillon, and Y. Galerne, J. Phys. II **5**, 1371 (1995).
[8] J. P. Michel, E. Lacaze, M. Alba, M. de Boissieu, M. Gailhanou, and M. Goldmann, Phys. Rev. E **70**, 011709 (2004).
[9] M. Kléman, O. D. Lavrentovich, and Y. A. Nastishin, *Dislocations and Disclinations in Mesomorphic Phases*, Vol. 12 of Dislocations in Solids (Elsevier Sciences, New York, 2004).
[10] J. P. Michel, E. Lacaze, M. Goldmann, M. Gailhanou, M. de Boissieu, and M. Alba, Phys. Rev. Lett. **96**, 027803 (2006).
[11] E. Lacaze, M. Alba, M. Goldmann, J. P. Michel, and F. Rieutord, Appl. Surf. Sci. **175-176**, 337 (2001).
[12] E. Perez and J. E. Proust, J. Phys. (France) Lett. **38**, 117 (1977).
[13] A. Buka, T. Toth Katona, and L. Kramer, Phys. Rev. E **49**, 5271 (1994).
[14] C. Blanc, Phys. Rev. E **64**, 011702 (2001).
[15] M. Vilfan, A. Mertelj, and M. Čopič, Phys. Rev. E **65**, 041712 (2002).
[16] E. Lacaze, M. Alba, M. Goldmann, J. P. Michel, and F. Rieutord, Eur. Phys. J. B **39**, 261 (2004).
[17] S. Bardon, R. Ober, M. P. Valignat, F. Vandenbrouck, A. M. Cazabat, and J. Daillant, Phys. Rev. E **59**, 6808 (1999).
[18] A. Sarlah and S. Žumer, Phys. Rev. E **60**, 1821 (1999).
[19] M. M. Wittebrood, D. H. Luijendijk, S. Stallinga, T. Rasing, and I. Musevic, Phys. Rev. E **54**, 5232 (1996).
[20] J. Thoen, H. Marynissen, and W. Van Dael, Phys. Rev. A **26**, 2886 (1982).
[21] J. G. Dash, H. Fu, and J. S. Wettlaufer, Rep. Prog. Phys. **58**, 115 (1995).
[22] L. J. Martinez-Miranda and Y. Hu, J. Appl. Phys. **99**, 113522 (2006).
[23] M. Cagnon and G. Durand, Phys. Rev. Lett. **70**, 2742 (1993).
[24] B. Zappone, Ph. Richetti, R. Barberi, R. Bartolino, and H. T. Nguyen, Phys. Rev. E **71**, 041703 (2005).